An Integrated Fast Battery Charger for Electric Vehicle

S. LACROIX, *Student Member, IEEE*, E. LABOURE, M. HILAIRET, *Member, IEEE*
Laboratoire de Génie Electrique de Paris (LGEP)/ SPEE-Labs ;
CNRS UMR8507; SUPELEC; Université Pierre et Marie Curie P6; Université Paris-Sud 11;
11, rue Joliot Curie, Plateau de Moulon F91192 Gif Sur Yvette Cedex
(samantha.lacroix, eric.laboure, mickael.hilairet)@lgep.supelec.fr

Abstract— **Under the requirements of reducing emissions, air pollution and achieving higher fuel economy, companies are developing electric, hybrid electric, and plug-in hybrid electric vehicles. However, the high cost of these technologies and the low autonomy are very restrictive. In this paper a new concept of fast on-board battery charger for Electric Vehicles (EVs) is proposed which uses the electric motor like filter and the same converter for charging and traction mode.**

Keywords-AC/DC converter; on-board battery charger; power factor correction (PFC); power electronics; electric vehicles (EVs) ; electric machines

I. INTRODUCTION

During the last years, hybrid electric vehicle (HEV) and electric vehicle (EV) technology seem to provide an effective solution of improving fuel economy, better performance, and lower emissions, compared with conventional vehicles [1]. Conversion of HEVs into plug-in hybrid electric vehicles (PHEVs) to reduce fuel consumption has been considered by the automotive industry. The conversion is achieved by either adding a high-energy battery pack or replacing the existing battery pack HEV to extend the all-electric range.

According to [2], the battery is one of the most critical components in the development of an EV. Its energy density, charging time, lifetime and cost are restricting practical applications. The charging time and lifetime of a battery depends on the characteristics of the battery charger and its usage. There are two kinds of chargers for the EV's application namely, on-board type and stand-alone type. "On-board" would be appropriate for night-time charging from a household utility outlet (slow charger), and "stand-alone", similar to a gas station, permits fast charging of the battery. The empty battery can also be changed by a full battery. The "stand-alone" solution presents some disadvantages which are:

- the high cost
- the risk of vandalism due to the accessibility of the battery recharging stations on public roads
- the cluttering in an urban environment.

In the state of art, there are a lot of topologies of battery charger for EV and HEV applications [2], [3], [4]. Fig. 1 shows

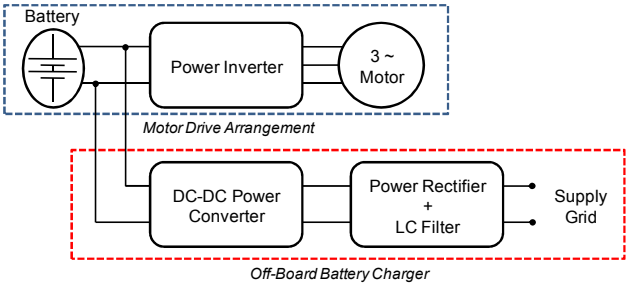

Figure 1. EV motor drive with off-board battery charger

the general architecture of an EV with an off-board battery charging system. Such architecture requires the use of two power converters, one for the vehicle propulsion and the other for charging the battery, which involved an additional cost for the system. In order to limit this main drawback, integrating the power electronics of the fast charger in the vehicle could be one of the solutions. Furthermore, the use of the power components of the EV motor drive could reduce the volume and the cost of battery chargers. For example, in [5], the proposed battery charger uses the power inverter of propulsion drive with an additional power rectifier and a LC filter which are easily placed close to the motor.

In the near future, the increasing use of EVs will have some consequences on the electric distribution system, like the harmonic pollution and the effects of the low power factor of the charger. So, AC outlet charging needs a battery charger with a power factor correction (PFC) [6].

In addition to power electronics, the technology of the electric motor plays a major role in the vehicle's dynamics and the type of power converter for controlling the vehicle.

This article deals with a new concept of fast on-board battery charger for Electric Vehicles (EVs) which uses the electric motor like filter and the same converter for charging and traction mode [7],[8].

This paper is organized as follows. In Section II, the concept of EV conversion and the structure of the proposed integrated converter are presented. Then, the charging mode is analyzed. The problematic is developed in Section III. Section IV shows the current controller design and the simulation results. Finally, Section V provides a conclusion and a discussion about future works.

978-1-4244-8218-4/10/$26.00 ©2010 IEEE

II. ANALYSIS OF THE PROPOSED CONCEPT

A. Electric Vehicle Principle

The development of EVs increases the use of embedded electronics and power electronics unlike conventional vehicles. Purpose of the new concept is to propose an innovative topology using the same expensive components for several independent functions, like traction mode and charger mode. This reduces the cost, the weight and the number of elements used. This concept is also applied in other applications like aeronautic or railway traction.

This kind of topology is called combination topology in [9] because it uses the drive motor's inverter as a battery charger unlike another topology that proposes an independent battery charger. However, solutions in [9] are suitable for a single-phase charger only.

In such topologies, the power unit can be used regardless of the operating mode - traction mode or charger mode - thanks to the bidirectional nature of power converters.

In each mode, only the power control is different. Moreover, in the charger mode, the winding inductances of the electrical motor are used as filter inductances for the controlled rectifier.

B. Proposed Converter

The power circuit schematic diagram of the proposed topology corresponding to the charging mode operation is shown in Fig. 2. It can be seen that the topology is composed of two three-phase PWM boost converters and a buck-boost chopper.

By controlling the two PFC (Power Factor Corrector) converters, the DC link voltage (U_{dc}) can be maintained at a defined constant value, and the AC current waveforms can be controlled in order to obtain the required power factor. The buck-boost chopper is controlled to regulate the battery charging current (i_{bat}) or voltage at the desired value.

In this topology, each phase of the AC grid is connected to two parallel PWM boost converters. This connection is realized through the midpoint of each winding of the electrical machine. In case of balanced current in each half windings of a given phase, the rotating magnetic field components at the stator level are eliminated. Therefore, there is no electromagnetic torque and the car remains stationary even if the brake is not pressed. Using the winding inductances of the electrical machine as a filter is conceptually very interesting but the control is different from a classical boost converter operating in a PFC mode.

C. Problem statement

Fig. 3 shows the structure of the converter which is almost similar to a classic three-phase PFC with the difference that the filtering inductors are replaced by the windings of the machine. Due to electric motor construction, a magnetic coupling exists between the six inductances. Because of this coupling, controlling the current in one of the winding could have consequences on the other currents. The current control is thus more complicated in this configuration [10]. Furthermore, another problem is due to the buried magnets rotor structure.

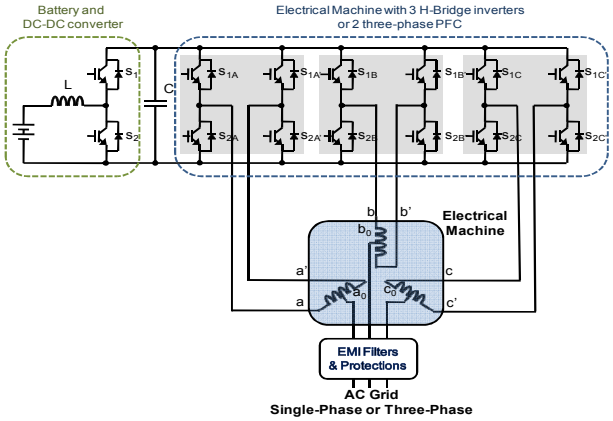

Figure 2. Power Circuit topology

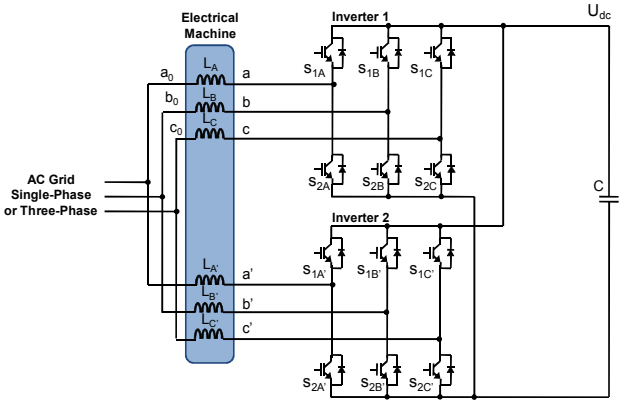

Figure 3. Equivalent circuit in charging mode of AC/DC converter with 2 three-phase PFC

For this kind of electrical machines, the inductances and mutual inductances values depend on the rotor position.

III. ELECTRIC MOTOR MODEL

In the AC/DC converter equivalent circuit, the electric motor is represented by six inductances. By construction, the number of stator windings is equal to the number of stator's teeth. This means that there are 12 windings at the stator. So a lot of coupling configurations series/parallel are possible. Two solutions allow midpoints connexions, as shown on Fig. 4. It is possible to see the magnetic field's repartition for the two connection types. In connection type 1 (Fig. 4-b), the fluxes in the two windings which are connected in parallel are different in a DC flux configuration. This leads in AC mode to a circulating current between the two windings even if no current is drawn from the machine. For connection type 2 (Fig. 4-c), the fluxes in the two windings connected in parallel are equal. This second connection mode is, therefore, the only viable one.

In charging mode, as there is no electromotive force, the motor can be represented only by an equivalent inductance matrix and by the stator winding resistance leading to the following equation:

$$V_m = R_s I_m + L_s I_m \, s \qquad (1)$$

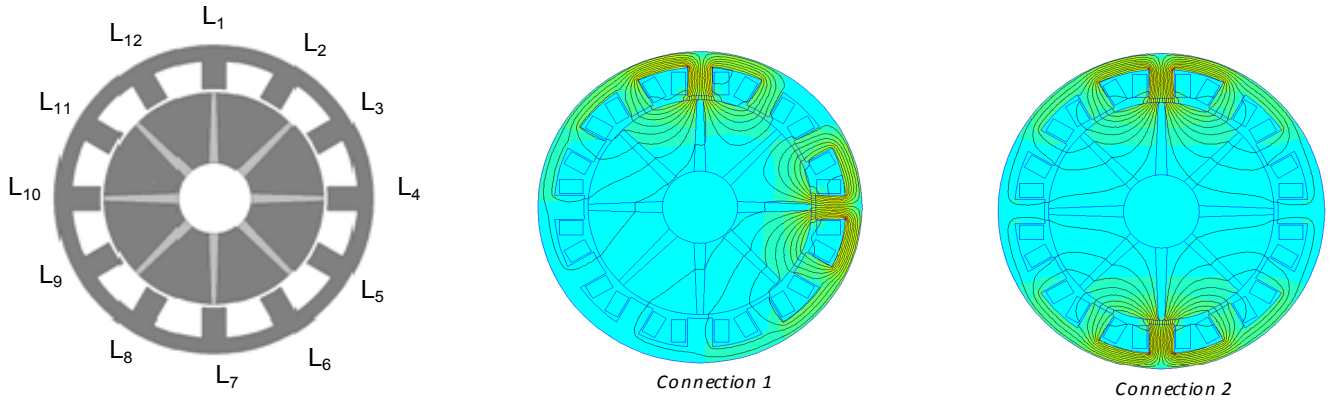

(a) *Position of the windings on the 2D machine's representation; Lines field for L_1 and L_4 supplied corresponding to connection 1; Lines field for L_1 and L_7 supplied corresponding to connection 2*

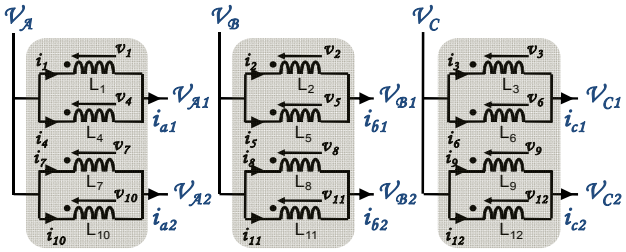

(b) *Connection 1*

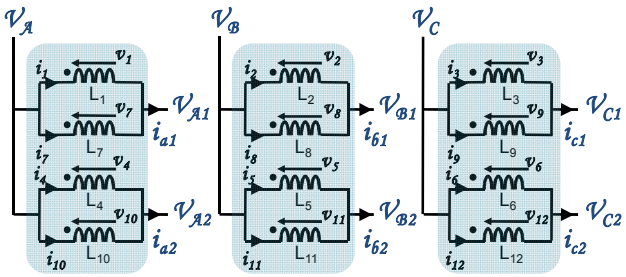

(c) *Connection 2*

Figure 4. Two kinds of connection of the windings

where Vm and Im represent respectively, the voltage vector and current vector of the motor windings, Rs is the stator's resistance matrix and Ls is the inductance matrix. In order to define the controller structure and parameters, the inductance matrix which represented the main part of the impedance must be identified. This is done by computed the magnetic fluxes in the electrical machine. These magnetic fluxes are linked to the motor currents by:

$$\psi_s = L_s I_m \tag{2}$$

Two methods based on finite element simulations can be used to identify the inductance matrix. In the first method, the connection mode of the elementary 12 stator windings is defined, giving the real 6 stator windings and then, the current in one of these 6 windings is imposed. The magnetic flux in each winding gives the first column of the 6x6 equivalent inductance matrix. The other terms are obtained by imposing successively the current in the other 5 windings. It is thus possible to determine each matrix inductance elements.

$$L_s = \begin{bmatrix} L_{11} & M_{12} & M_{13} & M_{14} & M_{15} & M_{16} \\ M_{21} & L_{22} & M_{23} & M_{24} & M_{25} & M_{26} \\ M_{31} & M_{32} & L_{33} & M_{34} & M_{35} & M_{36} \\ M_{41} & M_{42} & M_{43} & L_{44} & M_{45} & M_{46} \\ M_{51} & M_{52} & M_{53} & M_{54} & L_{55} & M_{56} \\ M_{61} & M_{62} & M_{63} & M_{64} & M_{65} & L_{66} \end{bmatrix} \tag{3}$$

In the second method, the global 12x12 inductance matrix corresponding to each winding parts is determined. This is done by successively imposing the current in each elementary part of the winding and calculating the magnetic flux in each winding. The dimension of the corresponding inductance matrix is 12x12. Then, according to the connections series/parallel, of the elementary windings, different reduction matrixes are defined leading to the following set of equations:

$$\begin{bmatrix} i_1 \\ \vdots \\ i_{12} \end{bmatrix} = [Y] \begin{bmatrix} v_1 \\ \vdots \\ v_{12} \end{bmatrix} \tag{4}$$

$$\begin{bmatrix} v_1 \\ \vdots \\ v_{12} \end{bmatrix} = [A] \begin{bmatrix} v_{A1} \\ v_{A2} \\ v_{B1} \\ v_{B2} \\ v_{C1} \\ v_{C2} \end{bmatrix} \qquad \begin{bmatrix} i_{a1} \\ i_{a2} \\ i_{b1} \\ i_{b2} \\ i_{c1} \\ i_{c2} \end{bmatrix} = [B] \begin{bmatrix} i_1 \\ \vdots \\ i_{12} \end{bmatrix} \tag{5}$$

$$\begin{bmatrix} v_{A1} \\ v_{A2} \\ v_{B1} \\ v_{B2} \\ v_{C1} \\ v_{C2} \end{bmatrix} = ([B][Y][A])^{-1} \begin{bmatrix} i_{a1} \\ i_{a2} \\ i_{b1} \\ i_{b2} \\ i_{c1} \\ i_{c2} \end{bmatrix} \tag{6}$$

where Y is the admittance matrix equal to $(R_s + L_s\,\mathrm{s})^{-1}$ (12x12), A and B representing transformation matrixes. The matrix A allows the transition between the 12 internal windings voltages to the 6 external voltages, and the matrix B links the 6 external currents to the 12 internal windings currents, note that $B^t = A$.

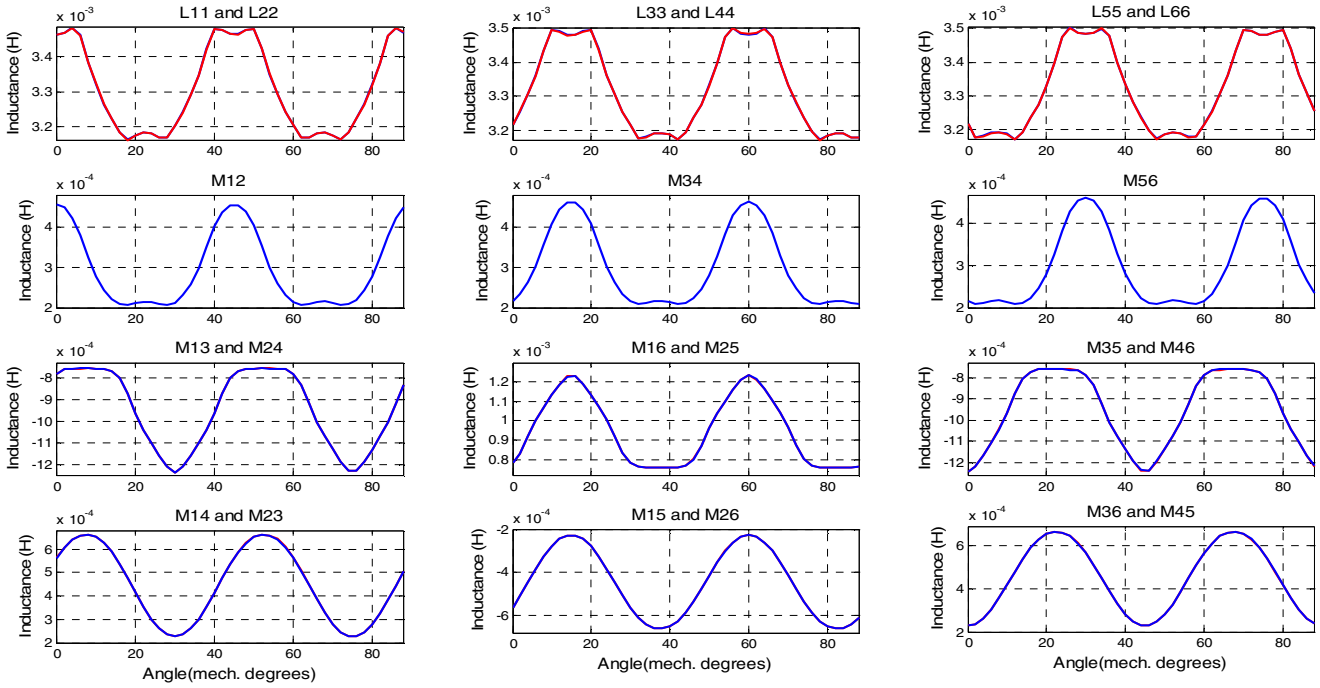

Figure 5. Parameters of the matrix inductance for different rotor's position

$$A = \begin{bmatrix} a & [0] & [0] \\ [0] & a & [0] \\ [0] & [0] & a \end{bmatrix} \quad \text{with} \quad a = \begin{bmatrix} 1 & 0 \\ 1 & 0 \\ 0 & -1 \\ 0 & -1 \end{bmatrix} \qquad (7)$$

The two methods give the same results. The second one is more general and allows investigations of the influence of connection mode on magnetic behavior.

Fig. 5 shows a small variation of the inductance value (about 10%) and a larger variation of the mutual inductances (about 100%) with the rotor position. In addition, the magnetic couplings between the 6 inductances are not negligible (for example 33% of the inductances value).

From these curves, Fast Fourier Transform has been performed in order to determinate the general expressions of inductances and mutual inductances as a function of the rotor position. We can notice that the waveforms are well restituted using a 5^{th} order polynomial function with position dependence. Doing the same for all the inductances and mutual inductances leads to determine analytical expressions for all elements of the electrical model. A comparison between the finite element simulation and the analytical expression is given in Fig. 6. These analytical expressions allow developing a model-based controller.

IV. Controller Design and Simulation Results

To evaluate the proposed converter, simulations have been performed for a single phase alimentation. In this single phase AC line configuration, only 8 motor windings are connected to the power inverter. The third H-bridge inverter is not used. The analytical model is integrated in a macroscopic representation of the system using MATLAB/Simulink and the SimPowerSystems Toolbox.

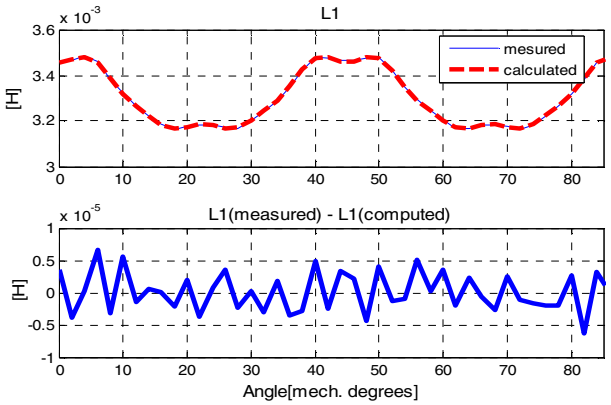

Figure 6. Comparaison between the finite element simulation and the analytical expression for the inductance L_{11}; analytique error between the both

The current control allows the absorption of a sinus current to the grid, and also ensures the current balancing in each winding of the motor in order to eliminate the rotating magnetic field. The schematic diagram of the AC single phase and the control block diagram are shown in Fig. 7. To eliminate the coupling induced by the magnetic behavior of the motor, the system of equation must be diagonalized.

A simplified control strategy for a particular polyphase motor without any saliency effects has been design. This machine leads to a circulating type inductance matrix L_{circ} such as:

$$L_{circ} = \begin{bmatrix} l & m & 0 & m \\ m & l & m & 0 \\ 0 & m & l & m \\ m & 0 & m & l \end{bmatrix}, \qquad (8)$$

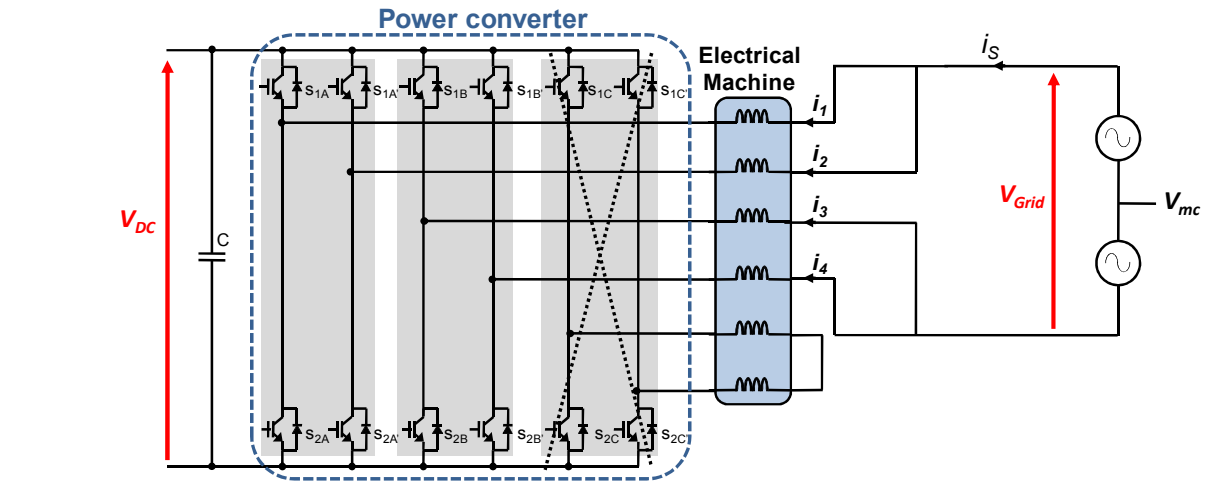

(a) Power circuit

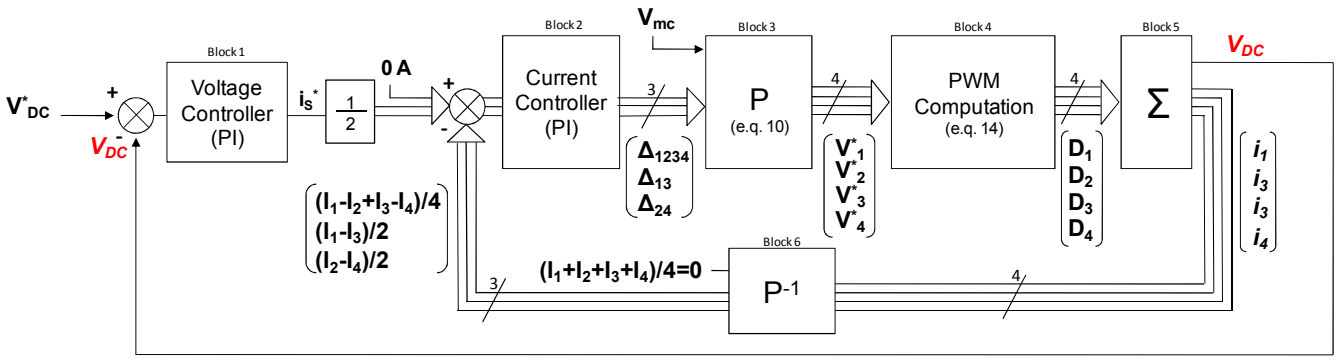

(b) Control block diagram

Figure 7. Power circuit in AC single phase charging mode and control block diagram associated

For such matrixes the diagonalization can be performed using the following expression:

$$L_{diag} = P^{-1} L_{circ} P, \tag{9}$$

$$\text{with, } P = \begin{bmatrix} 1 & 1 & 1 & 0 \\ 1 & -1 & 0 & 1 \\ 1 & 1 & -1 & 0 \\ 1 & -1 & 0 & -1 \end{bmatrix}. \tag{10}$$

Each column of P represents the eigenvectors of the inductance matrix. The use of matrix P leads to control the 3 currents can be independently controlled, using for example a simple Proportional and Integral (PI) controller.

The control principle using the transformation has been validated first on the particular polyphase machine characterized by (8). Then, in a second step, this machine's model has been replaced by the model of the real machine with a non negligible saliency effect. Furthermore, it has been possible to see that the eigenvectors corresponding to this synchronous motor change with position. Assuming that the rotor is motionless, the values of the inductance matrix are fixed. If the same base change is used like for the particular polyphase machine (eq. 10), the inductor matrix is not strictly diagonalized because couplings still exist but remain low.

The simulated power circuit is shown Fig. 7-a. Five quantities are measured, the DC link voltage and the windings currents (i_1, i_2, i_3, i_4). To keep the rotor stationary, the following conditions must be verified:

$$i_1 = i_2, i_3 = i_4 \text{ and } \; i_s = i_1 + i_2 = i_3 + i_4. \tag{11}$$

The control block diagram of the PWM boost converter is also shown in Fig. 7-b, where the external loop is the voltage loop and the internal one represents the current loop. Block 6 is the base change. Passing through this block, the inputs i_1, i_2, i_3, and i_4 become $(i_1\text{-}i_3)/2$, $(i_2\text{-}i_4)/2$ and $(i_1\text{-}i_2+ i_3\text{-}i_4)/4$ which are respectively compared where $i_s^*/2$, $i_s^*/2$ and zero.

After the PI controllers (block 2), the reference voltages are computed to return in the original base by performing a reverse transformation. This transformation needs the common mode voltage (V_m) i.e. $(V_1^* + V_2^* + V_3^* + V_4^*)/4$ that is imposed equal to $V_{DC}/2$ in the single phase configuration. The four output voltages of this block are computed as follows:

$$\begin{bmatrix} V_1^* \\ V_2^* \\ V_3^* \\ V_4^* \end{bmatrix} = P \begin{bmatrix} V_{mc} \\ \Delta_{1234} \\ \Delta_{13} \\ \Delta_{24} \end{bmatrix} \tag{12}$$

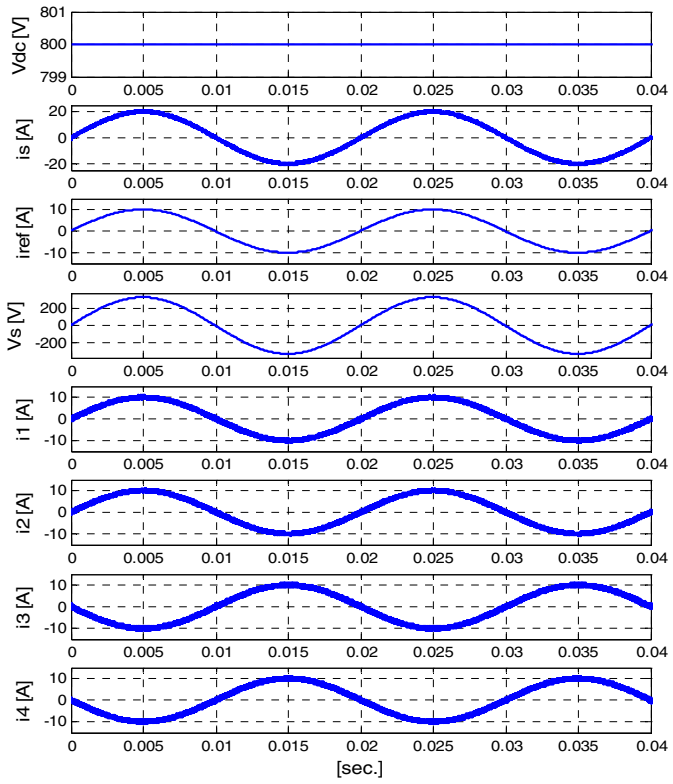

Figure 8. Unity power factor operation and current regulation of the boost converter. From top : dc link voltage; ac source current; current reference of inductance; ac source voltage; inductances currents

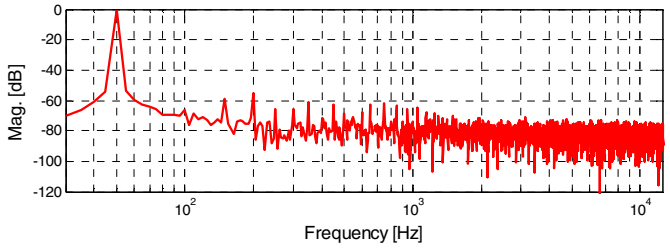

Figure 9. FFT of i_s current

where Δ_{1234}, Δ_{13}, Δ_{24} represent the output voltages of the PI controller. The control is base on 3 independents PI controllers and the expression is:

$$C(p) = K\frac{1+T_i p}{T_i p} \tag{13}$$

where T_i represents the integrator time constant and K the controller gain. Block 4 reconstructs the duty cycle references of the four half bridges using:

$$D_k = \frac{1}{V_{DC}}\left(V_k^* + \frac{V_s}{2}\right),\ k = 1,..,4 \tag{14}$$

The obtained signals D_k are then compared to a triangular ramp to generate the 4 PWM control signals.

Fig. 8 represents the currents regulation of the boost converter where the DC link voltage is assumed well regulated to his reference voltage equal to 800V. It can be noticed that the AC source current (i_s) is in phase with the source voltage (V_s) and also (i_s) has low harmonics content as shown in Fig. 9. The equality conditions (11) are verified and i_s is equal to twice the reference current in each phase. Although the inductance matrix is not perfectly diagonalizable, the AC source current is well regulated.

I. CONCLUSION

This paper has presented an embedded AC/DC charger for EV application. The proposed converter has been described and its particularity has been pointed out. Using electric motor as filtering inductance leads to develop particular electrical models. Using finite elements simulation, the linkage between inductances has been shown and evaluated. A general analytical model of the motor inductance matrix has been developed and a control strategy using this analytical model has been proposed and validated. Finally, this control strategy is under test in a prototype to validate our proposal.

ACKNOWLEDGMENT

This work was supported by the French automotive cluster MOVEO in a FUI program, through the project SOFRACI.

REFERENCES

[1] A. Emadi, Y. J. Lee, K. Rajashekara, "Power electronics and motor drives in electric, hybrid electric, and plug-in hybrid electric vehicles", *IEEE Transactions on Industrial Electronics*, vol. 55, no. 6, pp. 2237-2245, June 2008.

[2] S. K. Sul, S. J. Lee, "An integral battery charger for four-wheel drive electric vehicle", *IEEE Transactions on Industry Applications*, vol. 31, no. 5, pp. 1096-1099, September 1995.

[3] H. C. Chang, C. M. Liaw, "Development of a compact switched-reluctance motor drive for EV propulsion with voltage-boosting and PFC charging capabilities", *IEEE Transactions on Vehicular Technology*, vol. 58, no. 7, pp. 3198-3215, September 2009.

[4] P. Bajec, B. Pevec, D. Voncina, D. Miljavec, J. Nastran, "Extending the low-speed operation range of PM generator in automotive applications using novel AC-DC converter control", *IEEE Transactions on Industrial Electronics*, vol. 52, no. 2, pp. 436-443, April 2005.

[5] L. Solero, "Nonconventional on-board charger for electric vehicle propulsion batteries", *IEEE Transactions on Vehicular Technology*, vol. 50, no. 1, pp. 144-149, January 2001.

[6] Y. J. Lee, A. Khaligh, A. Emadi "Advanced integrated bidirectional AC/DCand DC/DC converter for plug-in hybrid electric vehicles", *IEEE Transactions on Vehicular Technology*, vol. 58, no. 8, pp. 3970-3980, October 2009.

[7] L. De Sousa, B. Bouchez, "Dispostif électrique combiné d'alimentation et de charge", French Patent WO 2010/057892 A1, Valeo Systèmes de Contrôle Moteur, May 2010.

[8] L. De Sousa, B. Bouchez, "Procédé et dispostif électrique combiné d'alimentation et de charge à moyens de compensation", French Patent WO 2010/057893 A1, Valeo Systèmes de Contrôle Moteur, May 2010.

[9] L. Shi, A. Meintz, M. Ferdowsi, "Single-phase bidirectional AC-DC converters for plug-in hybrid electric vehicle applications", *IEEE Vehicle Power and Propulsion Conference*, Harbin, China, September 2008.

[10] M. Le Bolloch, M. Cousineau, T. Meynard, "Current sharing control technique for interleaving VRMS using intercell transformers", *IEEE Power Electronics and Applications*, EPE'09, 13th Europeen Conference On, Barcelona, Spain, October 2009.